Spin-Crossover and Massive Anisotropy Switching of 5d Transition Metal Atoms on Graphene Nanoflakes

Igor Beljakov,[†] Velimir Meded,[†] Franz Symalla,[†] Karin Fink,[†] Sam Shallcross,[‡] Mario Ruben,[†] and Wolfgang Wenzel*,[†]

[†]Institute of Nanotechnology (INT), KIT, 76021, Karlsruhe, Germany

[‡]Friedrich Alexander Universität Erlangen Nürnberg (FAU), 91054, Erlangen, Germany

ABSTRACT: In spin crossover phenomena, the magnetic moment of a molecule is switched by external means. Here we theoretically predict that several 5d transition metals (TMs) adsorbed on finite graphene flakes undergo a spin crossover, resulting from multiple adsorption minima, that are absent in the zero dimensional limit of benzene and the two dimensional limit of graphene. The different spin states are stable at finite temperature and can be reversibly switched with an electric field. The system undergoes a change in magnetic anisotropy upon spin crossover, which facilitates read out of the spin state. The TM decorated nanoflakes thus act as fully controlled single ion magnetic switches.

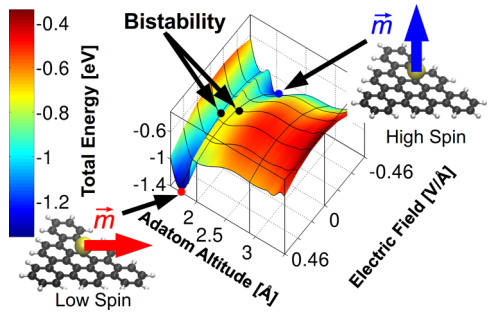

KEYWORDS: *Spin crossover, graphene nanoflake, bistability, magnetic anisotropy, transition metals, adsorption*

Spin crossover (SCO) phenomena, first observed in 1931,[1] have been studied for many years, motivated by both fundamental[2] and technological interest,[3,4] such as applications in magnetic storage devices or spintronics.[5] SCO has been observed in crystals of metal organic molecules[6] where the magnetic moment of the metal center in a ligand field can be externally switched between low spin (LS) and high spin (HS) state, for example, by temperature, light, pressure,[6] or magnetic field.[7] To date SCO has been observed in a number of 3d metal organic complexes, while for 4d and 5d transition metals (TM) the crystal field splitting induced by ligand cage is larger than the spin pairing energy, which effectively suppresses SCO.[7] SCO induced by external electric fields was recently observed on the single molecule level,[8] which opens new possibilities in spintronics[9] or quantum computing,[10] but has been confined to low temperatures.[8,11]

Here we investigate 5d TMs adsorbed on graphene flakes, because the π electron cloud may hybridize strongly with selected molecular orbitals of the TM.[12] Previous studies on the interaction of transition metal ions with graphene have already shown many interesting effects, such as electrically tunable electronic structure,[13] phonon mediated superconductivity,[14] and giant Rashba splitting.[15] More specifically, because of their strong spin−orbit coupling and high magnetic moment[16] 5d TMs adsorbed on graphene have displayed particularly interesting properties, such as high magneto crystalline anisotropy[17] and tunable quantum anomalous Hall effect.[18]

Geometry optimizations were performed using the VASP[19−21] ab initio simulation package with the Perdew−Burke−Ernzerhof (PBE) GGA exchange correlation functional[22] together with the empirical Grimme dispersion corrections (DFT D)[23] accounting for van der Waals forces. All single point calculations, in particular the calculation of the energy profiles of the azimuthal adsorption distances, were performed using TURBOMOLE[24,25] quantum chemistry package using again the PBE GGA exchange correlation functional and def2 TZVP basis sets.[26,27] Calculation of the spin−orbit interactions employed the two component dhf TZVP 2c basis set[28] in concert with the two component effective core potential dhf ecp 2c.[29] Where applicable, the results were verified against hybrid functionals (B3LYP[30−33] and TPSSH[34]) as well as to MP2,[35] showing satisfactory agreement. The magnetic anisotropy energy (MAE) is defined as the energy difference of the least and most favorable magnetization directions, comparing spin directions either perpendicular (out of plane) or the optimal in plane with the flake (in vs out of plane MAE, E_{IOP}), or the most versus the least optimal in plane spin direction (in plane MAE, E_{IP}). The term "flake" used throughout the paper stands for "nanoflake".

We have computed the electronic structure of 5d TM atoms on triangular graphene flakes with 6 (C_6, benzene), 18 (C_{18}, triphenylene), 36 (C_{36}, tribenzo(adg)coronene), and 90 (C_{90}) atoms, as well as for infinite graphene (C_∞) as a function of distance (Figure 1). The flake size is the parameter that effectively tunes the dimensionality of the system from zero (benzene) to two dimensions (graphene). Focusing initially on Os as an example we find a strong finite size effect that for C_{18}, C_{36}, and C_{90} results in the occurrence of secondary and tertiary

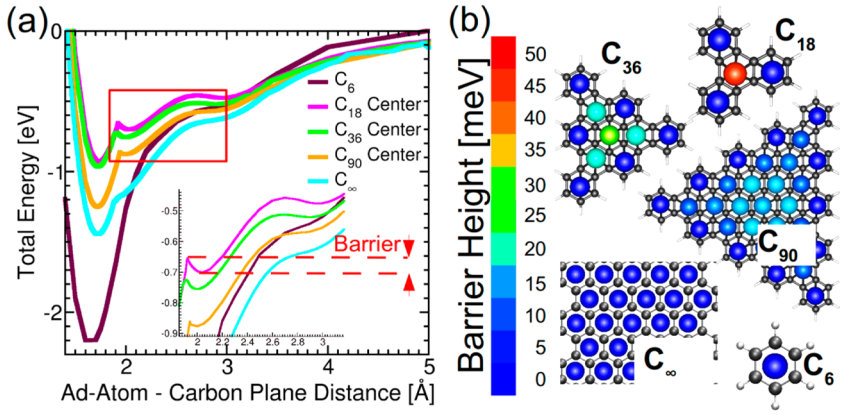

Figure 1. (a) Energy profiles of an Os adatom as a function of adsorption distance on the central sites of several graphene flakes. The inset in (a) illustrates the barrier between the first and second minimum. (b) Barrier height between the two minima of OS adsorbed on all possible sites for benzene (C_6), three different armchair triangulenes (C_{18}, C_{36}, C_{90}), and for the graphene sheet (C_∞).

minima of the energy as a function of distance to the flake (z_{min}) (Figure 1a). This effect exists neither for benzene nor for graphene, but only for small flakes. The C_{18} flake has the primary minimum at $z_{min(1)}$ = 1.74 Å, the most pronounced metastable secondary minimum at $z_{min(2)}$ = 2.04 Å, and a tertiary minimum at $z_{min(3)}$ = 2.95 Å. The primary and secondary minima are separated by a barrier of 45 meV = 522 K (see inset of Figure 1a), well above room temperature. The first two minima correspond to chemisorbed states with significant mixing of graphene and adatom orbitals, while the tertiary minimum is of van der Waals nature (see Supporting Information). We find that the existence of secondary minima is not limited to the central site of the flake, but occurs for essentially all sites on the C_{36} and C_{90} flakes with the exceptions of the sites on the edges including the apex, as seen in Figure 1b. The maximal barrier height strongly depends on the substrate size, varying from 20−45 meV for C_{90} and C_{18}, while the net charge on Os increases from 0.47e to 0.5e when going from C_{18} to C_{90} (see Supporting Information, Table S1 for details), permitting to fine tune the (meta)stability of the (secondary) primary minimum by choosing an appropriate substrate size.

The existence of two chemisorbed minima is often related to transitions in the electronic structure. For Os adsorbed on the central site of the C_{36} flake, we find that the total magnetization of the system changes from 1.56 μ_B (S = 1) for the primary minimum to 3.59 μ_B (S = 2) and 3.92 μ_B (S = 2) for the secondary and tertiary minima, respectively, with comparable changes for all other flakes and sites that feature a secondary minimum (see Supporting Information). In the order of the distance of the minima, the orbital population corresponds to $5d^8 6s^0$ (most filled d orbitals, henceforth called the "d" state), $5d^7\ 6s^1$ (one 6s orbital filled, "s" state) and $5d^6\ 6s^2$ (the physisorbed, "van der Waals" state, "v" state). The difference in adatom−flake distance for S = 1 and S = 2 minima of ∼0.3 Å is comparable to typical ligand cage expansions for LS HS transitions, for example, for $[Fe(bpp)_2]^{2+}$.[11]

As the distance changes, we observe a change in occupation of the 6s and (minority) 5d orbitals as shown in Figure 2 as a function of orbital character and energy (see also Supporting Information, Figures S1 and S2). We find that the 6s orbital hybridizes poorly, while the 5d orbitals hybridize well with the π system of the flake, reversing their order of occupation as a function of the adsorption distance. When going from the v

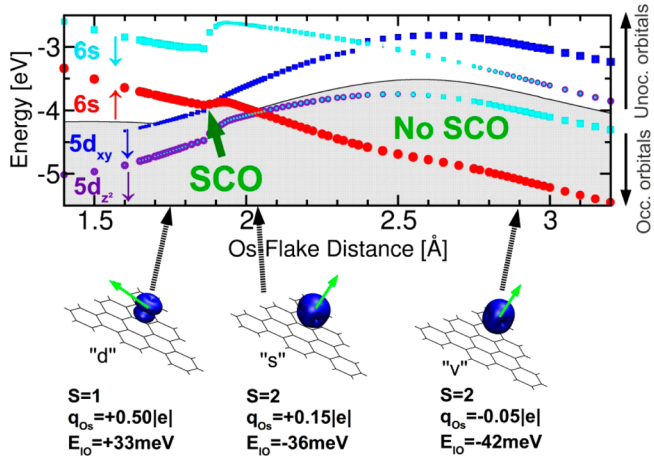

Figure 2. Energies of the orbitals of Os on C_{18} as a function of Os−C_{18} distance for four distinct orbitals: majority 6s as well as minority 6s, $5d_{z^2}$ and $5d_{xy}$. The gray area indicates occupied orbitals. Large dots indicate strong 5d or 6s character of the orbital respectively, small dots indicate hybridization. Hybridization from minority 6s to $5d_{z^2}$ occurs between 3 and 2.5 Å without any modification of the magnetization (v to s transformation, details in the text). Further reduction of the distance results in a spin flip between the majority 6s and the minority $5d_{xy}$ orbitals, corresponding to a SCO between a high spin (S = 2) s and low spin (S = 1) d state. The 6s orbitals hybridize only weakly with the flake states making them very energetically unfavorable at short distances, while 5d orbitals hybridize well (the dots become smaller at shorter distances). Below the graph: d, s and v states are depicted along with their magnetization (in blue). Both direction (change in sign of magnetic anisotropy energy, green arrow) and magnitude (S = 2 to S = 1) of the magnetization along with the Os atom charge transfer (+0.15|el to +0.5 el) change considerably upon SCO.

state to the d state via the s state we first have a transformation caused by hybridization between minority 6s and minority $5d_{z^2}$ orbital, with no change of the magnetization (v to s), followed by 6s majority electron flipping over to the $5d_{xy}$ minority orbital (the 5d majority orbitals are fully occupied) resulting in a SCO transition (s to d) that modifies the system from a high spin (S = 2) to a low spin (S = 1) state. In the d state, the system exhibits a stronger charge transfer from the adatom to the substrate that leads to added stability; q_{Os} in Figure 2 changes from −0.05 |el for the v state to +0.5 |el for the d state.

This change in orbital hybridization suggests that an electric field perpendicular to the flake plane may couple differentially to the orbitals occupied in the different minima and hence affect their energies differently. In Figure 3, we show the

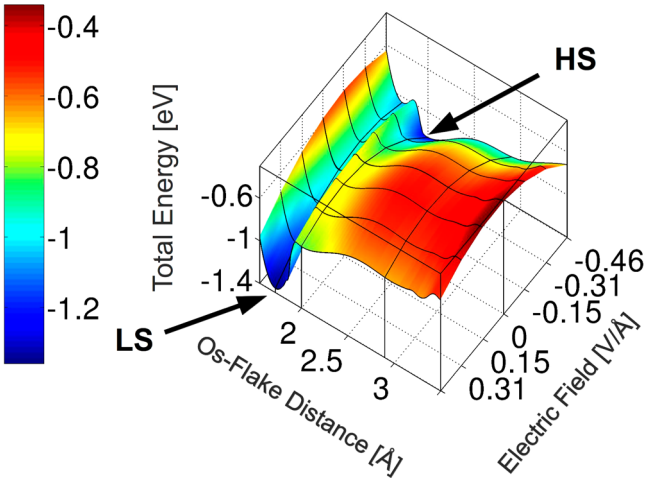

Figure 3. Energy profiles of Os adatom as a function of adatom−C_{36} flake distance as well as different perpendicular electric field. For high (negative) positive filed the most stable state is (s, HS) d, LS permitting switching between the states. At zero field the barrier between the states is 30 meV, clearly higher than room temperature (25 meV).

modulation of the energy profiles, again using the Os adsorbed on the central site of a C_{36} flake, as a function of the applied field. We find that the energetic order of the minima changes with distance, stabilizing the s state minimum at 2.0 Å over the d state minimum at 1.72 Å for applied external fields larger than −0.3 V/Å. Thus, application of an external field permits us to switch the magnetization of the system from S = 1 (LS) to S = 2 (HS), which will remain stable at room temperature even when the field is removed due to the existence of a barrier of up to 30 meV = 348 K between the s and the d state for the zero field curve. Application of a field in the opposite direction reduces the barrier between the states, strongly stabilizing the d state minimum and permits to switch the system back to the d state from the s state, establishing a mechanism for spin crossover of 5d TMs adsorbed on graphene flakes. We note that this mechanism is not limited to a particular flake size or adsorbate position, but occurs for all nonedge sites on the C_{18}, C_{36}, and C_{90} flake and may be present for other shapes as well. Because neither benzene (C_6) nor infinite graphene have a barrier in the zero field limit, these systems feature reversible spin switching but not bistable spin crossover, which is in agreement with earlier observations.[18] The electric field has a very strong effect on the charge transfer between the adatom and the flake (see Supporting Information, Figure S3, for details); for an external electric field pointing from the flake to the Os atom, the charge transfer increases from +0.50|e| to +0.65|e|, which stabilizes the more hybridizing state (d). The opposite effect, that is, stabilizing s/v occurs when the external field is inverted, which also reduces the charge transfer to +0.32|e|.

Large magnetic anisotropies have been reported for TM adsorption on planar systems like benzene and graphene.[36,37] We have therefore investigated the existence of an easy axis in the zero field ground state (LS, S = 1) as a function of position for the C_{36} and C_{90} flakes. When comparing the energies of systems in the d state with spin directions the optimal in plane versus the out of plane direction, we find a strong preference to align the spin directions with the plane of the flake ("easy plane"). For C_{90}, the anisotropy is varying from 13 to 23 meV depending on the position on the flake as shown in Figure 4a.

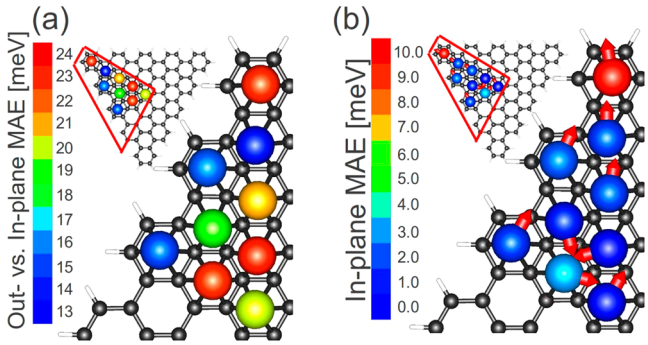

Figure 4. MAE for C_{90} decorated with an Os adatom at the symmetry inequivalent hollow sites (see the insets). (a) In versus out of plane MAE (E_{IOP}) along with (b) in plane MAE, where the most pronounced values are at the apex with E_{IOP} = 22.9 and $E_{IP} \approx 10$ meV. The red arrows in (b) indicate the preferable in plane magnetization direction pinning and their length is proportional to the corresponding E_{IP}.

We also find that the preferred direction in the plane is pinned and depends in a nontrivial manner on the position of the atom on the flake as illustrated in Figure 4b. We note that the pinning is an edge induced effect (symmetry lowering) and is absent for adsorption on either benzene or graphene.

We also find that the spin crossover transition is followed by massive change in magnetization direction. For Os adsorbed on the central position of C_{36}, the in plane spin direction is stabilized by E_{IOP} = +33 meV in the d state, which changes to −36 meV for the s state, that is, the magnetic moment switches out of the plane and attains its strongest out of plane stabilization in the v state (−42 meV), where only crystal field splitting is present (confirmed by sharply diminishing net charge on Os as a function of distance, see insets of Figure 2). The change in sign for magnetic anisotropy is attributed to change in the occupation of 5d orbitals and results from the low symmetry of the ligand "cage", that is, the flake.

For Os adatom adsorption on C_{90}, we find that hollow sites directly at the edge of the flakes are more preferable than sites in the center of the flake, which is in accord with previous findings on graphene ribbons[38] and lattice defects on graphene[39] and graphite.[40] The barrier heights between neighboring hollow sites are in the order of several hundred millielectronvolts,[41] making the nonedge sites metastable at room temperature. Edge functionalization may prove to be important for added stability of the system and as such will be addressed in future work. As shown in Table 1, the large magnetic anisotropy energy can be observed throughout the 5d series, in some cases followed by massive anisotropy switch. Likewise, one can see that the bistability behavior is not a unique feature of Os. However, the details, for example, difference between HS and LS, switching site position (bistability is observed at the apex sites for W, Ta, and Re), and so forth, seem to be adatom specific, further confirming that by the choice of the adatom and the flake size the SCO effect can be tuned in desired direction.

Table 1. Bistability Properties of 5d TM Elements[a]

element	bistable Site	d_{Prim} [Å]	d_{Sec} [Å]	$E_{IOP,Prim}$ [meV]	$E_{IOP,Sec}$ [meV]	barrier [eV]	S_{Prim}	S_{Sec}
Hf	edge	2.05	1.90	9.5	[b]	0.021	1	1
Ta	apex	1.84	1.72	12.0	[b]	0.002	3/2	1/2
W	apex	1.71	3.00	11.0	2.9	0.300	1	3
Re	apex	1.68	3.10	3.7	2.7	0.560	1/2	5/2
Os	center	1.72	2.00	34.3	37.1	0.030	1	2
Ir	center	1.97	2.00	33.9	13.2	0.031	3/2	3/2

[a] d_{Prim} and d_{Sec} are the adatom−flake distances for two stable and metastable minima respectively, while $E_{IOP,Prim}$ and $E_{IOP,Sec}$ are the corresponding in versus out of plane MAE. Barrier heights are displayed, as well. Additionally, the spin value of the two states is shown in the last two columns. Bistability is always present and often accompanied by change of magnetization and massive anisotropy switching (see W for example). [b] – not calculated (barriers assumed to be too small).

In conclusion, by using first principles methods we discovered a spin crossover effect for 5d transition metal centers on graphene armchair flakes that is not present for either benzene or fully extended graphene substrates. Application of experimentally achievable external electric fields perpendicular to the flake plane permits switching between the high and low spin states, which are metastable at room temperature. Because of planar symmetry of the system, which is far lower than in molecular context frequently encountered in (distorted) octahedral ligand cages, this SCO is accompanied by a massive magnetic anisotropy change where the easy magnetization axis rotates 90° upon the SCO transition. This feature generates for two significant technological advantages: the transition can be observed with standard magnetic recording[9,42] and or observed directly using scanning tunneling spectroscopy and similar approaches.[43] Because the TM remains confined to the flake, controlled deposition of arrays of finite graphene flakes with 5d TM adsorption may yield single ion magnetic switches that may be used at room temperature in a number of interesting technological applications, opening avenues for further miniaturization of magnetic storage devices, or creating spintronic devices, using the spin crossover effect for spin filtering[44,45] in the underlying substrate.

■ ASSOCIATED CONTENT

● Supporting Information

The Supporting Information contains following chapters: understanding of the nature of Os−flake bonding by analyzing the charge transfer; orbital structure analysis by observing the orbital occupation and energy; influence of the electric field on the Os−flake charge transfer; validity of the Grimme approach; and reliability of magnetic moments predictions. This material is available free of charge via the Internet at http://pubs.acs.org.

■ AUTHOR INFORMATION

Corresponding Author

*E mail: wolfgang.wenzel@kit.edu.

Author Contributions

The calculations were performed by I.B., F.S., K.F., and V.M., the project was planned and supervised by S.S., M.R., and W.W. The manuscript was written through contributions of all authors.

I.B. and V.M. contributed equally.

Notes

The authors declare no competing financial interest.

■ ACKNOWLEDGMENTS

This work was supported by the FP7 ICT project MMM@HPC (contract number: 261594) and DFG WW1863/21 1. The authors would like to acknowledge Dr. Romain Danneau for fruitful discussions. V.M. acknowledges Ferdinand Evers. S.S. acknowledges support from ESF under EUROCORES program CRP Graphic RF (DFG Grant PA 516/8 1) and the Special Priority Program "Graphene'" (DFG Grant PA 516/9 1) and by the Collaborative Research Center SFB 953.

■ ABBREVIATIONS

SCO, spin crossover; TM, transition metal; LS, low spin; HS, high spin; MAE, magnetic anisotropy energy; E_{IOP}, in versus out of plane magnetic anisotropy energy; E_{IP}, in plane magnetic anisotropy energy

■ REFERENCES

(1) Cambi, L.; Szegö, L. *Ber. Dtsch. Chem. Ges., A and B* **1931**, *64* (10), 2591−2598.
(2) Grimm, R. *Nature* **2005**, *435*, 1035−1036.
(3) Halder, G.; Kepert, C.; Moubaraki, B.; Murray, K.; Cashion, J. Guest Dependent Spin Crossover in a Nanoporous Molecular Framework Material. *Science* **2002**, *298*, 1762−1765.
(4) Létard, J. F.; Guionneau, P.; Goux Capes, L., Towards Spin Crossover Applications. In *Spin Crossover in Transition Metal Compounds III*; Springer: Berlin Heidelberg, 2004; Vol. *235*, pp 221−249.
(5) Baadji, N.; Piacenza, M.; Tugsuz, T.; Sala, F. D.; Maruccio, G.; Sanvito, S. *Nat. Mater.* **2009**, *8* (10), 813−817.
(6) Breuning, E.; Ruben, M.; Lehn, J. M.; Renz, F.; Garcia, Y.; Ksenofontov, V.; Gütlich, P.; Wegelius, E.; Rissanen, K. *Angew. Chem., Int. Ed.* **2000**, *39* (14), 2504−2507.
(7) Gütlich, P.; Goodwin, H. *Spin Crossover in Transition Metal Compounds I*; Springer: New York, 2004; Vol. *I*, p 341.
(8) Miyamachi, T.; Gruber, M.; Davesne, V.; Bowen, M.; Boukari, S.; Joly, L.; Scheurer, F.; Rogez, G.; Yamada, T. K.; Ohresser, P.; Beaurepaire, E.; Wulfhekel, W. *Nat. Commun.* **2012**, *3*, 938.
(9) Bogani, L.; Wernsdorfer, W. *Nat. Mater.* **2008**, *7* (3), 179−186.
(10) Timco, G. A.; Carretta, S.; Troiani, F.; Tuna, F.; Pritchard, R. J.; Muryn, C. A.; McInnes, E. J. L.; Ghirri, A.; Candini, A.; Santini, P.; Amoretti, G.; Affronte, M.; Winpenny, R. E. P. *Nat. Nanotechnol.* **2009**, *4* (3), 173−178.
(11) Meded, V.; Bagrets, A.; Fink, K.; Chandrasekar, R.; Ruben, M.; Evers, F.; Bernand Mantel, A.; Seldenthuis, J. S.; Beukman, A.; van der Zant, H. S. J. *Phys. Rev. B* **2011**, *83* (24), 245415.
(12) Chan, K. T.; Lee, H.; Cohen, M. L. *Phys. Rev. B* **2011**, *84* (16), 165419.
(13) Brar, V. W.; Decker, R.; Solowan, H. M.; Wang, Y.; Maserati, L.; Chan, K. T.; Lee, H.; Girit, C. O.; Zettl, A.; Louie, S. G.; Cohen, M. L.; Crommie, M. F. *Nat. Phys.* **2011**, *7* (1), 43−47.
(14) Profeta, G.; Calandra, M.; Mauri, F. *Nat. Phys.* **2012**, *8* (2), 131−134.

(15) Marchenko, D.; Varykhalov, A.; Scholz, M. R.; Bihlmayer, G.; Rashba, E. I.; Rybkin, A.; Shikin, A. M.; Rader, O. *Nat. Commun.* **2012**, *3*, 1232.
(16) Stepanyuk, V. S.; Hergert, W.; Wildberger, K.; Zeller, R.; Dederichs, P. H. *Phys. Rev. B* **1996**, *53* (4), 2121−2125.
(17) Ouazi, S.; Vlaic, S.; Rusponi, S.; Moulas, G.; Buluschek, P.; Halleux, K.; Bornemann, S.; Mankovsky, S.; Minár, J.; Staunton, J. B.; Ebert, H.; Brune, H. *Nat. Commun.* **2012**, *3*, 1313.
(18) Zhang, H.; Lazo, C.; Blügel, S.; Heinze, S.; Mokrousov, Y. *Phys. Rev. Lett.* **2012**, *108* (5), 056802.
(19) Kresse, G.; Hafner, J. *Phys. Rev. B* **1993**, *47* (1), 558−561.
(20) Kresse, G.; Furthmüller, J. *Comput. Mater. Sci.* **1996**, *6* (1), 15−50.
(21) Kresse, G.; Furthmüller, J. *Phys. Rev. B* **1996**, *54* (16), 11169−11186.
(22) Perdew, J. P.; Burke, K.; Ernzerhof, M. *Phys. Rev. Lett.* **1996**, *77* (18), 3865−3868.
(23) Grimme, S. *J. Comput. Chem.* **2006**, *27* (15), 1787−1799.
(24) TURBOMOLE V6.3.1 2011, a development of University of Karlsruhe and Forschungszentrum Karlsruhe GmbH, 1989−2007; TURBOMOLE GmbH: Karlsruhe, 2007.
(25) Ahlrichs, R.; Bär, M.; Häser, M.; Horn, H.; Kölmel, C. *Chem. Phys. Lett.* **1989**, *162* (3), 165−169.
(26) Weigend, F.; Häser, M.; Patzelt, H.; Ahlrichs, R. *Chem. Phys. Lett.* **1998**, *294* (1−3), 143−152.
(27) Weigend, F.; Ahlrichs, R. *Phys. Chem. Chem. Phys.* **2005**, *7* (18), 3297−3305.
(28) Weigend, F.; Baldes, A. *J. Chem. Phys.* **2010**, *133* (17), .
(29) Peterson, K. A.; Figgen, D.; Dolg, M.; Stoll, H. *J. Chem. Phys.* **2007**, *126* (12), .
(30) Becke, A. D. *J. Chem. Phys.* **1993**, *98* (7), 5648−5652.
(31) Lee, C.; Yang, W.; Parr, R. G. *Phys. Rev. B* **1988**, *37* (2), 785−789.
(32) Vosko, S. H.; Wilk, L.; Nusair, M. *Can. J. Phys.* **1980**, *58* (8), 1200−1211.
(33) Stephens, P. J.; Devlin, F. J.; Chabalowski, C. F.; Frisch, M. J. *J. Phys. Chem.* **1994**, *98* (45), 11623−11627.
(34) Tao, J.; Perdew, J. P.; Staroverov, V. N.; Scuseria, G. E. *Phys. Rev. Lett.* **2003**, *91* (14), 146401.
(35) Haase, F.; Ahlrichs, R. *J. Comput. Chem.* **1993**, *14* (8), 907−912.
(36) Sargolzaei, M.; Gudarzi, F. *J. Appl. Phys.* **2011**, *110* (6), 064303.
(37) Xiao, R.; Fritsch, D.; Kuz'min, M. D.; Koepernik, K.; Richter, M.; Vietze, K.; Seifert, G. *Phys. Rev. B* **2010**, *82* (20), 205125.
(38) Sevinçli, H.; Topsakal, M.; Durgun, E.; Ciraci, S. *Phys. Rev. B* **2008**, *77* (19), 195434.
(39) Cretu, O.; Krasheninnikov, A. V.; Rodríguez Manzo, J. A.; Sun, L.; Nieminen, R. M.; Banhart, F. *Phys. Rev. Lett.* **2010**, *105* (19), 196102.
(40) Lee, S. M.; Lee, Y. H.; Hwang, Y. G.; Hahn, J. R.; Kang, H. *Phys. Rev. Lett.* **1999**, *82* (1), 217−220.
(41) Zólyomi, V.; Rusznyák, A.; Kürti, J.; Lambert, C. J. *J. Phys. Chem. C* **2010**, *114* (43), 18548−18552.
(42) Wernsdorfer, W. Classical and Quantum Magnetization Reversal Studied in Nanometer Sized Particles and Clusters. In *Handbook of Advanced Magnetic Materials*; Liu, Y., Sellmyer, D., Shindo, D., Eds.; Springer: New York, 2006; pp 77−127.
(43) Miyamachi, T.; Schuh, T.; Markl, T.; Bresch, C.; Balashov, T.; Stohr, A.; Karlewski, C.; Andre, S.; Marthaler, M.; Hoffmann, M.; Geilhufe, M.; Ostanin, S.; Hergert, W.; Mertig, I.; Schon, G.; Ernst, A.; Wulfhekel, W. *Nature* **2013**, *503* (7475), 242−246.
(44) Garcia Lekue, A.; Balashov, T.; Olle, M.; Ceballos, G.; Arnau, A.; Gambardella, P.; Sanchez Portal, D.; Mugarza, A. *Phys. Rev. Lett.* **2014**, *112* (6), 066802.
(45) Yang, H. X.; Hallal, A.; Terrade, D.; Waintal, X.; Roche, S.; Chshiev, M. *Phys. Rev. Lett.* **2013**, *110* (4), 046603.